Hydrogen bonding in supercritical water: A Monte Carlo simulation

ARTICLE *in* CHEMICAL PHYSICS LETTERS · DECEMBER 1994

Impact Factor: 1.9 · DOI: 10.1016/0009-2614(94)01245-8

2 AUTHORS:

Andrey G. Kalinichev
École des Mines de Nantes
117 PUBLICATIONS **2,926** CITATIONS
SEE PROFILE

Jay Bass
University of Illinois, Urbana-Champai…
213 PUBLICATIONS **4,916** CITATIONS
SEE PROFILE

ELSEVIER

23 December 1994

Chemical Physics Letters 231 (1994) 301–307

CHEMICAL PHYSICS LETTERS

Hydrogen bonding in supercritical water: a Monte Carlo simulation

A.G. Kalinichev [1], J.D. Bass

Department of Geology, University of Illinois at Urbana-Champaign, 1301 W. Green St., 245 Natural History Bldg., Urbana, IL 61801, USA

Received 28 July 1994; in final form 27 September 1994

Abstract

A detailed analysis of hydrogen bonding in supercritical water is made from Monte Carlo simulations along the 773 K isotherm over a wide range of pressures from 10 to 10000 MPa. It is shown that an energetic definition of H-bonding is much more effective in separating H-bonded and non-bonded molecular pairs than the widely used geometric definition, whereas a combination of both may be yet preferable at high pressures. Compared to H bonds in liquid water, the H bonds at 773 K are, on average, 10% weaker, 5% longer, and more bent. The quantitative characteristics of supercritical H bonds remain almost invariant over the entire pressure range studied.

1. Introduction

Supercritical water (i.e. water at temperatures and pressures above the critical point, $T_c = 647$ K, $P_c = 22.1$ MPa) has recently become a subject of growing scientific interest due to new technological applications [1,2], as well as because of its crucial role in a variety of geological processes [3,4]. Due to the large compressibility of supercritical fluid, small changes in pressure can produce substantial changes in density which, in turn, affect diffusivity, viscosity, dielectric, and solvation properties, thus dramatically influencing the kinetics and mechanisms of chemical reactions in water. Monte Carlo (MC) and molecular dynamics (MD) computer simulations of supercritical water [5–10] have significantly improved our understanding of the molecular mechanisms responsible for the complex behavior of thermodynamic and structural properties of this interesting chemical medium.

Hydrogen bonding, arising as a consequence of the charge distribution on individual water molecules, is one of the important phenomena affected by changes of temperature and pressure under supercritical conditions. For a quantitative analysis of the H bonding in computer simulations, various geometric definitions of H bonds are often used. They are based on the requirement that one or several internal coordinates of a pair of water molecules be within a certain specified range of values [11–14]. By the energetic definition of a hydrogen bond [15], two molecules are considered H bonded if the interaction energy between them is less than a given negative threshold. This definition has also been successfully applied to analyze the temperature and pressure effects on the H bond distributions in liquid water [16–20].

In this Letter, we present an analysis of hydrogen bonding in supercritical water using two simple geometric and energetic criteria. We propose intermolecular energy–distance distributions as an effective

[1] On leave from: Institute of Experimental Mineralogy, Russian Academy of Sciences, 142432 Chernogolovka, Moscow District, Russian Federation.

SSDI 0009-2614(94)01245-8

way to visualize the picture of H bonding in water. We also show that the simple geometric criterion of H bonding, most commonly used in the analysis of both computer simulations (e.g. Ref. [6]) and experimental measurements [21], is much less satisfactory under supercritical conditions than the energetic criterion, while a combination of both seems preferable, especially at higher pressures.

2. Monte Carlo simulations

The MC simulations were performed for a system of $N=216$ water molecules using a conventional NPT-ensemble algorithm [22] described in detail elsewhere [8]. Water molecules were interacting via the effective site–site pair potential TIP4P [18], which uses the experimental rigid geometry of the monomer (OH bond length $=0.9572$ Å and $\angle$HOH$=104.52°$), and has four interaction sites: three on the nuclei, and one on a point M located on the bisector of the HOH angle at a distance of 0.15 Å from the oxygen towards the hydrogens. The hydrogens are assumed to have charges of 0.52 e, compensated by the charge -1.04 e on M. The total interaction energy for a pair of molecules consists of the Coulomb interactions between the charged sites and a Lennard-Jones interaction between the oxygen atoms, with the parameters $\sigma=3.154$ Å and $\epsilon/k=78.1$ K in conventional LJ units [18].

Eight thermodynamic states were simulated along the 773 K supercritical isotherm in a pressure range from 10 to 10000 MPa, thus sampling a very wide density range between 0.03 and 1.67 g/cm^3. Simulated values of density, configurational enthalpy, isobaric heat capacity, isothermal compressibility, and thermal expansivity are listed in Table 1, along with values calculated using the equation of state of Saul and Wagner [23] for comparison. For each thermodynamic state the properties were averaged over 10^7 MC configurations with another 5×10^6 configurations generated on the preequilibration stage. The convergence of all the properties was monitored during the simulations and the statistical uncertainties (Table 1) were calculated by averaging over 50 smaller parts of the total Markov chain of configurations.

The present results are consistent with our previous simulations [8] for a smaller system ($N=64$), demonstrating the remarkable ability of the TIP4P intermolecular potential to accurately reproduce the thermodynamic properties of supercritical water over very wide ranges of pressures or densities, while indicating at the same time that the critical point for this water model is located about 50–70° lower than observed experimentally.

This qualitatively correct behavior of the simulated supercritical isotherm allows us to analyze in more detail the density dependence of local geometric and energetic arrangements of water molecules leading to hydrogen bonding.

3. Hydrogen bond distributions

The atom–atom radial distribution functions, g_{OO}, g_{OH} and g_{HH}, for 773 K and 1000 MPa (where supercritical water has the same density as normal liquid water, ≈1 g/cm^3), are shown in Fig. 1 (dashed lines). Solid lines in Fig. 1 represent the results of simulations at 298 K and 0.1 MPa. Cumulative coordination numbers, calculated as

$$n_{OO}(r)=4\pi\rho\int_0^r r^2 g_{OO}(r)\,dr$$

are also shown in Fig. 1a for both low-temperature and high-temperature conditions.

Fig. 1 demonstrates that the structure of water changes dramatically at supercritical temperature, even at liquid-like density. The characteristic second maximum of $g_{OO}(r)$ at ≈4.5 Å, reflecting the tetrahedral ordering of water molecules due to hydrogen bonding, is completely absent under these conditions, and a pronounced minimum of the distribution appears in its place. The comparison of the $g_{OO}(r)$ and $n_{OO}(r)$ functions at low and supercritical temperatures shows a significant redistribution of nearest neighbors from the 'hydrogen-bonding' regions of ≈2.7–2.9 Å and ≈3.8–5.0 Å to the 'non-bonding' region of ≈3.1–3.8 Å. As discussed previously [24], it is precisely the pairs of molecules at intermediate distances which are primarily responsible for repulsive interactions in liquid water, and these repulsions obviously increase under supercritical conditions. At the same time, the number of clos-

Table 1
Thermodynamic properties of supercritical TIP4P water along the 773 K isotherm

	P (MPa)							
	10	30	50	100	300	1000	3000	10000
ρ (g cm^{-3})	0.0306(1) [a]	0.1115(5)	0.214(1)	0.435(2)	0.724(2)	0.997(1)	1.275(1)	1.6401(5)
	0.0305 [b]	0.1151	0.2571	0.5285	0.7719	1.0140	1.2616	1.6662
H_{conf} (kJ mol^{-1})	3.82(2)	−1.43(5)	−5.93(6)	−12.03(7)	−14.81(4)	−8.71(4)	13.79(4)	86.18(5)
	4.36	−0.875	−7.40	−14.71	−16.56	−9.73	13.88	84.07
C_p (J mol^{-1} K^{-1})	44.0(5)	70(2)	90(3)	93(3)	65(2)	60(1)	57(1)	59(1)
	46.7	78(4)	131.2	100.1	71.9	62.5	61.3	65.6
$\kappa\times10^3$ (MPa^{-1})	108(2)	44(2)	24(1)	7.6(5)	0.96(5)	0.24(1)	0.066(2)	0.0201(4)
	109.39	47.07	32.69	5.424	0.850	0.205	0.0674	0.0283
$\alpha\times10^5$ (K^{-1})	183(5)	340(20)	420(20)	345(20)	107(5)	51(2)	24.6(9)	13.7(6)
	178.3	379.0	708.7	328.1	106.7	44.04	25.91	22.68

[a] Statistical uncertainties in the last significant figures are given in parentheses.
[b] In the second row the values calculated from the equation of state [23] are given for comparison as 'experimental'.

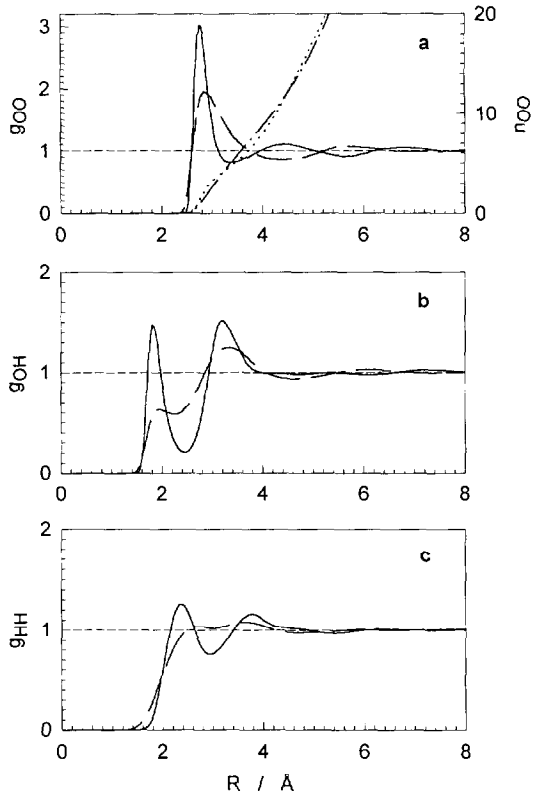

Fig. 1. Atom–atom radial distribution functions for liquid (298 K and 0.1 MPa; solid lines) and supercritical (773 K and 1000 MPa; dashed lines) water. The density in both thermodynamic states is the same (see Table 1). Dotted and dash-dotted lines represent cumulative coordination numbers for the low-temperature and high-temperature states, respectively.

est neighbors at distances up to ≈3.3 Å (the first minimum of $g_{OO}(r)$ in normal liquid water) remains unchanged.

The sharp first peak and following deep minimum of $g_{OH}(r)$ for normal liquid water (at ≈1.8 Å and ≈2.4 Å, respectively) become much less pronounced under supercritical conditions (Fig. 1b). These two characteristic features of $g_{OH}(r)$ observed in computer simulations, as well as experimentally [25], are the basis of a simple geometric definition of a hydrogen bond, whereby the bond is taken to exist between a pair of water molecules whose respective O and H atoms are separated by less than 2.4 Å. This criterion can provide convenient quantitative estimates of the number of H bonds experienced by an individual molecule under various thermodynamic conditions via integration under $g_{OH}(r)$ up to the chosen threshold distance (e.g., Ref. [6]).

Another purely energetic definition of hydrogen bonding was first introduced by Stillinger and Rahman [15], and is based on the analysis of pair energy distributions. These functions represent the distribution of energies between every pair of water molecules and are easily obtainable from computer simulations. Fig. 2a shows such functions for the same two thermodynamic states considered in Fig. 1. Most interactions involve pairs of distant molecules, resulting in the main peak of the distribution around 0 kJ/mol. However, in liquid water (solid line in Fig. 2a),

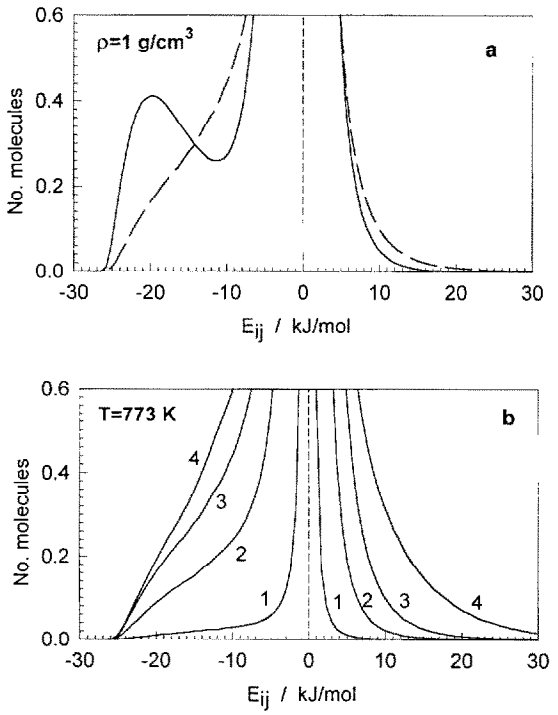

Fig. 2. Normalized distributions of pair interaction energies (dimerization energies) in liquid and supercritical water. (a) Temperature dependence at a constant density of 1 g/cm³. (——) 298 K; (– – –) 773 K. (b) Pressure (density) dependence along the 773 K isotherm. (1) 10 MPa; (2) 100 MPa; (3) 1000 MPa; (4) 10000 MPa.

there exists a low-energy peak due to hydrogen-bonded neighbors. The minimum at about −10 kJ/mol is most commonly associated with the energetic cutoff (E_{HB}) for hydrogen bonding [15–20].

Under the supercritical conditions of the present study the temperature is already too high to obtain this low-energy peak, but a distinct shoulder is clearly seen at the same range of energies, indicating the persistence of hydrogen bonding. Pair energy distributions for the 773 K isotherm over a wide pressure range are shown in Fig. 2b. As pressure (density) decreases, the distribution becomes narrower with higher maxima (beyond the scale in Fig. 2), because relatively more pairs of molecules are found at large intermolecular distances, with a near-zero interaction energy. However, the low-energy hydrogen bonding shoulder is still present in these distributions. It has been previously shown [15,17] that variation of the energetic cutoff value, within reasonable limits, does not qualitatively affect the picture of hydrogen bonding in liquid water, which remains remarkably similar for a number of water potentials used in simulations [15–20]. Thus, adopting $E_{HB} = -10$ kJ/mol universally for all thermodynamic states provides us with another simple criterion to quantitatively estimate the number of H bonds experienced by an individual water molecule at various temperatures and pressures.

In order to better visualize hydrogen bonding we propose to use combined distance–energy distributions, as shown in Fig. 3. Each point on the surface of such a distribution represents the relative probability of finding a hydrogen atom of a molecule i at a distance $R_{O...H}$ from the oxygen atom of a molecule j, with a specified interaction energy between the molecules of E_{ij}. It is clear from Fig. 3 that for normal liquid water either geometric (G) or energetic (E) criteria allow us to successfully distinguish H-bonded pairs of molecules from the non-bonded ones, with the former being represented by the distinct low-energy short-distance peak on the distance–energy dis-

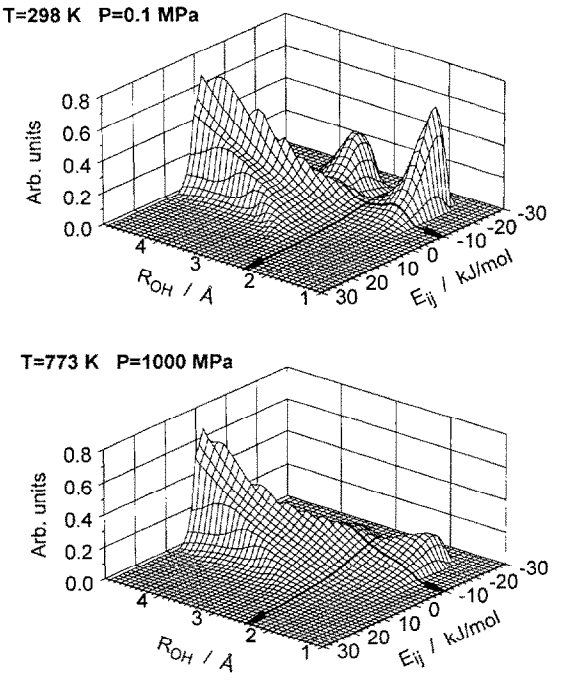

Fig. 3. Normalized intermolecular O...H distance–energy distribution functions for liquid and supercritical states at a density of ≈1 g/cm³.

tribution surface. Only 7% of molecular pairs considered bonded by the E criterion are excluded by the other criterion. This number is 13% for the G criterion.

Under supercritical conditions, the situation becomes much more complicated even at an equivalent density of 1 g/cm^3 (Fig. 3, bottom). Of molecular pairs satisfying the criterion E, 23% are considered non-bonded by the G criterion, and this number is as high as 37% for molecular pairs satisfying G, but not E criterion. It is important to emphasize that at supercritical temperature the non-overlapping 'tails' of the distance–energy distributions extend far beyond the chosen threshold values of HB energy and distance. Some of the molecular pairs counted as bonded in geometric terms can even have positive (repulsive) interaction energy, thus being obviously non-bonded in any reasonable physical sense. On the other hand, molecular pairs counted as H bonded in energetic terms can have an O...H separation as high as 3.0 Å. A purely geometric definition of H bonds can, obviously, be made more selective by introducing additional constraints on the interatomic separations and relative orientations of the interacting molecular pairs [11–14]. However, this compromises the simplicity of the criteria by increasing the number of free parameters in the analysis.

It is clear from the above brief discussion that the simultaneous application of both E and G criteria yields a better definition of the hydrogen bond. The pressure dependences of the average number of H bonds per water molecule $\langle n_{HB} \rangle$ according to all three (E, G, and E+G) definitions are shown in Fig. 4. For normal liquid water (open symbols) all definitions give very close results. However, for the supercritical 773 K isotherm, the results satisfying only E or G criteria start to diverge at $\approx$300 MPa, with the latter giving twice as many H bonds per water molecule at the highest pressure studied (10000 MPa), and without any indication of a possible maximum at higher pressure. The average value of $\approx$6 H bonds per water monomer given by the G criterion seems a significant overestimation, if one considers that every monomer can form two bonds as a proton – donor and two bonds as a proton – acceptor, and thus can be involved in a total of four 'ideal', minimally distorted, H bonds.

The superiority of the energetic criterion over the

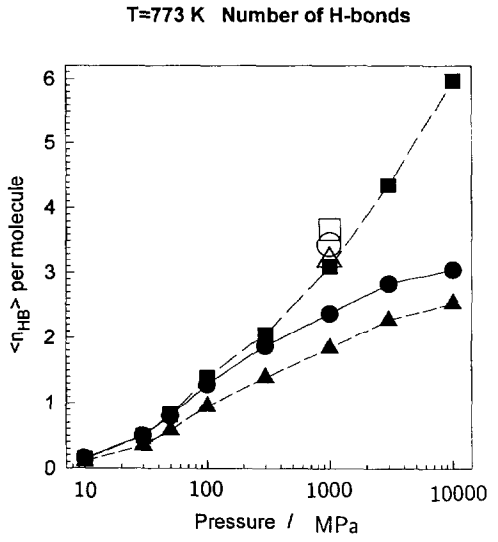

Fig. 4. Pressure dependence of the average number of H bonds per water molecule according to geometric (■), energetic (●), and combined criteria (▲). Open symbols for normal liquid water (298 K and 0.1 MPa) are plotted at 1000 MPa, where the density of supercritical water is also $\approx$1 g/cm^3.

geometric one at high pressures (or densities) is yet more clearly demonstrated in Fig. 5, where percent distributions of molecules involved in a given number of H bonds (numbers at the curves) is plotted against pressure. Here again, both criteria behave almost identically up to $\approx$300 MPa. However, at the highest pressure, application of the G criterion alone results in 8% of molecules involved in 8(!) H bonds, with another 22%, 32%, and 25% of molecules involved in 7, 6, and 5 bonds, respectively. On the other hand, the application of the E criterion alone results in much more reasonable distribution with only 2% of molecules involved in 6 H bonds and another 9% in 5 bonds, while most molecules have 2, 3, or 4 bonds. It is interesting to note that application of the E criterion results in values fairly close to the ones obtained using stricter E+G criterion (circles and triangles in Fig. 4, respectively), with both pressure dependences showing a reasonable trend towards saturation of $\langle n_{HB} \rangle$ at high pressures.

Average energy U_{HB}, distance $R_{O...H}$, and angles $\theta = \angle$O–H...O and $\phi = \angle$H...O–H of H bonds obtained from the present simulations by the application of the E+G criterion are presented in Table 2. The energy of the H bonding is divided into Coulom-

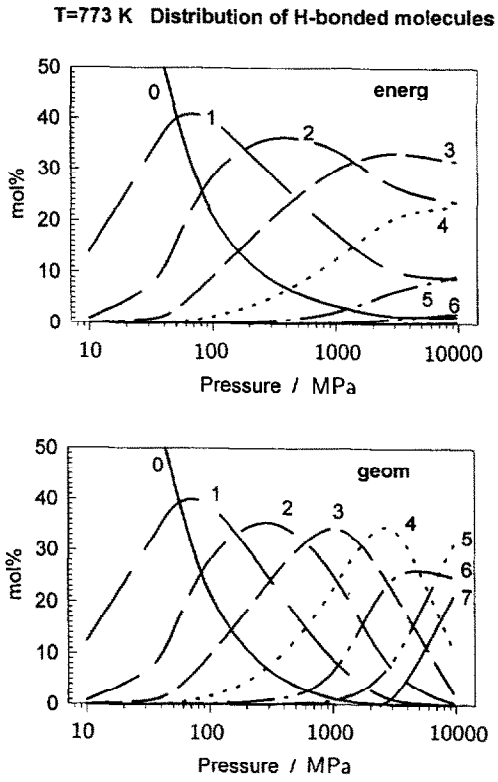

Fig. 5. Distribution of molecules involved in a given number of H bonds (numbers on the curves) in supercritical water at 773 K over a wide range of pressures (densities), according to energetic and geometric criteria.

bic and Lennard-Jones contributions, according to the definition of the TIP4P interaction potential. As expected, the average HB distance decreases with increasing pressure along the isotherm, bringing about an increase of the repulsive LJ contribution to the pair interaction energy. At the same time however, the Coulombic contribution decreases, resulting in average total energy of H bonding being almost invariant over the entire pressure range. Although some smooth variation of the average HB angles θ and ϕ is clearly observable, they too remain almost constant over the pressure range studied here. The same can be said about the angular distributions of H bonds (not presented here for brevity). Thus, we may conclude that the increase of temperature from ambient 298 K to supercritical 773 K affects the characteristics of H bonding in water much more dramatically than the changes in pressure within the range from 10 to 10000 MPa (corresponding to density changes from 0.03 to 1.67 g/cm^3) along the supercritical isotherm. Compared to H bonds in normal liquid water, the H bonds at 773 K are almost 2 kJ/mol weaker, have longer O...H bond distances by $\approx$0.1 Å, and are about 10° less linear. These findings confirm and extend considerably the observations of Jorgensen and Madura [19,20] on the effects of temperature and pressure on hydrogen bonding in water.

Acknowledgement

The study has been performed on a IBM RS/6000 workstation granted to the authors in the framework of IBM's Shared University Research (SUR) program and has been supported by the NSF grant EAR-

Table 2
Average parameters of hydrogen bonding in liquid and supercritical TIP4P

	T (K)								
	298	773	773	773	773	773	773	773	773
	P (MPa)								
	0.1	10	30	50	100	300	1000	3000	10000
$\langle U_{HB} \rangle$ (kJ mol^{-1})	−18.03	−16.48	−16.48	−16.46	−16.39	−16.31	−16.21	−16.03	−15.67
$\langle U_{Coulomb} \rangle$ (kJ mol^{-1})	−24.19	−20.80	−20.83	−20.85	−20.88	−21.08	−21.49	−22.13	−23.45
$\langle U_{LJ} \rangle$ (kJ mol^{-1})	6.16	4.33	4.36	4.39	4.49	4.77	5.28	6.09	7.79
$\langle R_{O...H} \rangle$ (Å)	1.928	2.077	2.071	2.066	2.058	2.046	2.028	2.006	1.968
$\langle \theta \rangle$ (deg)	160.1	148.9	149.7	150.3	150.9	151.3	151.1	150.2	148.6
$\langle \phi \rangle$ (deg)	99.7	94.2	95.1	95.6	96.2	96.2	95.8	95.0	94.1

9305071 and by the grant 94-03-08476-c from the Russian Basic Research Foundation.

References

[1] J.M.H. Levelt-Sengers, Intern. J. Thermophys. 11 (1990) 399.
[2] R.W. Shaw, T.B. Brill, A.A. Clifford, C.A. Eckert and E.U. Franck, Chem. Eng. News 69, No. 51 (1991) 26.
[3] D.L. Norton, Ann. Rev. Earth Planet. Sci. 12 (1984) 155.
[4] K.L. Von Damm, Ann. Rev. Earth Planet. Sci. 18 (1990) 173.
[5] A.G. Kalinichev, Intern. J. Thermophys. 7 (1986) 887.
[6] R.D. Mountain, J. Chem. Phys. 90 (1989) 1866.
[7] P.T. Cummings, H.D. Cochran, J.M. Simonson, R.E. Mesmer and S. Karaborni, J. Chem. Phys. 94 (1991) 5606.
[8] A.G. Kalinichev, Z. Naturforsch. 46a (1991) 433; 47a (1992) 992.
[9] A.G. Kalinichev and K. Heinzinger, in: Advances in physical geochemistry, Vol. 10. Thermodynamic data: systematics and estimation, ed. S.K. Saxena (Springer, Berlin, 1992) ch. 1.
[10] J. Brodholt and B. Wood, J. Geophys. Res. 98B (1993) 519.
[11] A.C. Belch, S.A. Rice and M.G. Sceats, Chem. Phys. Letters 77 (1981) 455.
[12] M. Mezei and D.L. Beveridge, J. Chem. Phys. 74 (1981) 622.
[13] G. Pálinkás, P. Bopp, G. Jancsó and K. Heinzinger, Z. Naturforsch. 39a (1984) 179.
[14] A.C. Belch and S.A. Rice, J. Chem. Phys. 86 (1987) 5676.
[15] F.H. Stillinger and A. Rahman, J. Chem. Phys. 57 (1972) 1281.
[16] W.L. Jorgensen, Chem. Phys. Letters 70 (1982) 326.
[17] D.C. Rapaport, Mol. Phys. 50 (1983) 1151.
[18] W.L. Jorgensen, J. Chandrasekhar, J.D. Madura, R.W. Impey and M.L. Klein, J. Chem. Phys. 79 (1983) 926.
[19] W.L. Jorgensen and J.D. Madura, Mol. Phys. 56 (1985) 1381.
[20] J.D. Madura, B.M. Pettitt and D.F. Calef, Mol. Phys. 64 (1988) 325.
[21] P. Postorino, R.H. Tromp, M.-A. Ricci, A.K. Soper and G.W. Neilson, Nature 366 (1993) 668.
[22] M.P. Allen, and D.J. Tildesley, Computer simulation of liquids (Oxford Univ. Press, Oxford, 1987).
[23] A. Saul and W. Wagner, J. Phys. Chem. Ref. Data 18 (1989) 1537.
[24] H. Tanaka and I. Ohmine, J. Chem. Phys. 87 (1987) 6128.
[25] A.K. Soper and M.G. Phillips, Chem. Phys. 107 (1986) 47.